

Type of the Paper: Article

# Electrokinetic Characterization of Natural Stones Coated with Nanocomposites for the Protection of Cultural Heritage

Marco Roveri <sup>1,\*</sup>, Simona Raneri <sup>2</sup>, Sabrina Bianchi <sup>4</sup>, Francesca Gherardi <sup>1</sup>, Valter Castelvetro <sup>3,4,\*</sup>, Lucia Toniolo <sup>1,4</sup>

<sup>1</sup> Dipartimento di Chimica, Materiali e Ingegneria Chimica “Giulio Natta”, Politecnico di Milano, Piazza Leonardo da Vinci, 32, 20133, Milan, Italy; marco.roveri@polimi.it, fra.gherardi@gmail.com, lucia.toniolo@polimi.it; e-mail@e-mail.com

<sup>2</sup> Dipartimento di Scienze della Terra, Università di Pisa, Via Santa Maria, 53, 56126, Pisa, Italy; simona.raneri@unipi.it

<sup>3</sup> Dipartimento di Chimica e Chimica Industriale, Università di Pisa, Via G. Moruzzi, 13, 56124, Pisa, Italy; sabrinab@dcc.i.unipi.it, valter.castelvetro@unipi.it

<sup>4</sup> National Interuniversity Consortium of Materials Science and Technology (INSTM), Firenze, Italy

\* Correspondence: valter.castelvetro@unipi.it; tel.: +39-320-711-1008; marco.roveri@polimi.it.

**Featured Application:** Characterization of the quality and homogeneity of surface treatments for non-porous and porous substrates

**Abstract:** Protective coatings, in recent years also from nanocomposite formulations, are commonly applied onto architectural stone and stone artefacts, mainly to prevent absorption into the porous stone structure of condensed water and dissolved atmospheric pollutants. While standard protocols are available to assess a coating's performance, understanding the response of the coating-stone system is a complex task, due to the interplay of various factors determining the overall behaviour. Characterization techniques allowing to correlate the extent and nature of surface modification upon treatment with the most relevant physical properties (i.e. water absorption and surface wettability) are thus of great interest. Electrokinetic analysis based on streaming current measurements, thanks to its sensitivity towards even minor changes in the surface chemical composition, may fulfil such requirement. Indeed, by involving the interaction with a testing aqueous electrolyte solution, this technique allows to probe not only the outer surface but also the outermost layer of the pore network, which plays a crucial role in the interaction of the stone with condensed atmospheric water. In this work a correlation was found between the extent of surface modification, as determined by streaming current measurements, surface wettability and capillary water absorption of 6 coating-lithotype combinations (3 lithotypes and 2 nanocomposites).

**Keywords:** natural stones; alkylalkoxysilane; nanocomposite coatings; surface modification; zeta potential; streaming current

## 1. Introduction

The protection of natural stones used in historical architecture is generally carried out through the application of suitable water-repellent coatings, which prevent the capillary absorption of liquid water into the porous network of the substrate, thereby limiting the related deterioration phenomena [1]. Since the effectiveness of these coatings mostly relies on their ability to modify the interaction of the treated surface with water, understanding the extent of surface modification, both in terms of effective surface coverage and change of chemical properties, is a key issue for the prediction of protective efficacy [2].

The effects of a hydrophobic coating on the surface properties can be studied at the macroscopic level by evaluating the behaviour of the treated stone with respect to established physical parameters, among which capillary water absorption and surface wettability have the highest relevance. Complementary to this, electron and atomic force microscopy give an insight into treatment-induced changes of the stone surface morphology at the micro- and nano-scale [3,4], while EDX and FTIR spectroscopies may allow to detect the presence and the surface distribution of a coating material through the observation of atomic [5] and molecular spectra [6], respectively.

However, linking information at the microscale, e.g. from observation of stone surface morphology, to macroscopic effects in terms of physical behaviour can be especially arduous. In the first place, natural stones are heterogeneous systems with high complexity and variety in terms of microstructure, mineralogical and chemical composition. Secondly, the wide range of coating materials that may be used in stone protection show markedly different properties as well. Thus, the main factors responsible for the overall behaviour of the system towards water may be very difficult to identify, all of which makes a prediction of the effectiveness of a coating material an arduous or impossible task [7]. Besides that, for porous solids such as natural stones, the very concept of “surface” defies a clear-cut definition; in fact, the effective surface area interacting with external agents and/or with a protective coating material upon its application, includes both the macroscopic outer surface and the outermost part of the pore network, insofar as the pore walls may also be involved in such interaction. Thus, upon application of a water repellent treatment, its contribution to the modification of surface texture and properties depends on the product penetration, reactivity and distribution. Unfortunately, surface analysis of stones by microscopy techniques does not allow a complete description and quantification of the topology of the pore network representative of the inner microstructure [8], thus only limited and possibly misleading information about the real distribution of the treating material can be attained through this way. As further shortcomings, the spectroscopic detection of silicon-based products, which are currently the class of materials most widely employed for natural stone treatment [9], is generally difficult on stones containing quartz or clay minerals, while the detection of the presence and homogenous distribution of a coating layer based on morphology can be critical on any stone if the applied product generates nanometric layers resulting in barely visible modifications of the stone surface [10].

In view of better understanding the extent of surface modification of stones after the application of a protective product or formulation, a potentially useful contribution may come from electrokinetic analysis based on streaming potential/streaming current measurements. As far as macroscopic and non-conductive solid materials are concerned, these measurements have established themselves as valuable tools for investigating the chemical properties of solid/liquid interfaces [11] and, in particular, for pinpointing the contribution of the surface chemical composition to the electrostatic component of the overall interaction with an electrolyte-carrying aqueous medium. Moreover, it must be considered that, in the case of a porous substrate, an aqueous medium is also likely to interact with the outermost layer of the pore network and, since the latter may be significantly modified upon application of a protective treatment, electrokinetic analysis may allow a more complete and far-reaching characterization of treatment-induced changes of surface properties.

The theoretical foundations of electrokinetic techniques were laid more than one century ago by von Smoluchowski [12], who introduced the fundamental concept of zeta potential and described its measurement by drawing on Helmholtz’s theory of electrical double layer (EDL). Zeta potential is defined as the electric potential at the slip plane of a solid/electrolyte interface, the slip plane being a virtual surface separating the layer of molecules and ions immobilized by adsorption onto the solid surface (roughly the Stern layer) from the rest of the EDL where they are free to move. Its magnitude reflects the net charge density at the solid surface and the charge distribution in the EDL, and is an indicator of the ability of the solid material to establish electrostatic interactions with charged species (ions of the electrolyte, colloidal particles) coming close to its surface. In a streaming current or a streaming potential measurement, a macroscopic laminar flow of the electrolyte fluid tangential to the solid surface is induced by a hydrostatic pressure gradient, resulting in a net charge flow if the

EDL presents an unbalanced ionic composition, as it is the case when the zeta potential is not zero. This convective transport of mobile ions in the direction of the liquid flow, which is called streaming current, can be detected directly by measuring the electric current between two non-polarizable electrodes positioned up- and downstream, respectively, with an electrometer of sufficiently low internal resistance. Alternatively, the electric potential generated by the convective charge transport, or streaming potential, can be measured between the same two electrodes with a high-input impedance voltmeter. According to the Smoluchowski model, if the EDL is sufficiently thin and the flow is laminar, the zeta potential is directly proportional to the derivative of streaming current ( $I_s$ ) with respect to the applied pressure difference ( $\Delta p$ ), according to eq. 1:

$$\zeta = \frac{dI_s}{d\Delta p} \cdot \frac{\eta \cdot \kappa}{\varepsilon_0 \cdot \varepsilon} \cdot R, \quad (1)$$

where  $\kappa$ ,  $\varepsilon$  and  $\eta$  are the electrical conductivity, dielectric constant and viscosity of the bulk electrolyte solution, respectively,  $\varepsilon_0$  is the vacuum permittivity and  $R$  is the electrical resistance of the streaming channel.

Currently, the electrokinetic characterization via streaming current/streaming potential measurements is the most straightforward technique for measuring the zeta potential of macroscopic solid surfaces and it has been used for a broad range of materials, including paper, textiles, membranes, biomaterials, soil and minerals [13-19]. Electrokinetic measurements provide a mean for studying such different phenomena as the adsorption of ionic species on inorganic substrates or of proteins on surfaces of biological interest, as well as the extent of modification of the substrate surface and its time-dependent evolution [20]. Furthermore, zeta potential can be an extremely useful parameter in the description of granular or fibrous materials and of porous ones such as e.g. semipermeable membranes [21] and natural stones [22], especially in connection with their behaviour in aqueous media as a function of pH [23,24]. Nevertheless, there is still a nearly complete lack of studies concerning the characterization of natural stone surfaces [25] and of the effect on the surface zeta potential resulting from treatment applications [26].

The aim of the present study is to explore the potential of electrokinetic analysis as a tool to better understand the changes occurring at the surface of natural stones after the application of protective coatings. For this purpose, the results of streaming current measurements are compared with the observed changes in the stone-water interaction as assessed by two commonly employed parameters for the evaluation of protective effectiveness, namely surface wettability and water absorption by capillarity [9]. It is worth stressing out that a multiplicity of factors contributes to the effectiveness of a protective coating, particularly if nanocomposite in its formulation. Among them, the porosity, pore size distribution and roughness of the substrate; the intrinsic hydrophobicity of the coating material and its ability to produce a uniform and continuous (but not occluding) layer sheathing both the outer stone surface and the outermost pore walls.

The present study was focused on devising an electrokinetic-based parameter suited for the semi-quantitative estimation of the degree of surface modification, allowing a prediction of the overall behaviour of a given coating-stone system. For this purpose, three lithotypes (natural stones used in ancient architectures) with different microstructural and mineralogical properties and two different coating formulations were considered. The formulations, consisting of liquid dispersions of different organosilica matrix precursors combined with titania nanoparticles, were developed in the framework of the EU-funded NanoCathedral project, dealing with the set-up and testing of innovative nanocomposite materials for the conservation of European architectural heritage. Their protective effectiveness was evaluated by static contact angle and water absorption measurements, performed on the lithotypes before and after the application of the coating formulations. In addition, electrokinetic characterization of untreated and treated stones and of the coatings obtained by casting onto a non-porous reference substrate was performed. The existence of well-defined correlations between the changes induced by the coatings on the electrokinetic properties and the reduction of surface wettability and of capillary water absorption in the treated stones was investigated.

## 2. Materials and Methods

### 2.1 Lithotypes

The stone specimens (5x5x2 cm blocks, figure 1) belong to three different lithotypes: Apuan marble, Balegem limestone and Obernkirchen sandstone. Apuan marble (from Carrara, Italy), an extremely compact metamorphic rock, is almost pure calcite; Balegem stone is a limestone from the Ghent region (Belgium), quite compact in texture despite featuring many millimetre-sized cavities; it is composed of siliceous clastic arenite in a sparitic cement (calcite and dolomite); Obernkirchen stone is a fine-grained porous sandstone (from Lower Saxony, Germany) and its composition includes mainly quartz with some kaolinite, feldspars and dolomite [27]. The calcite and dolomite content of the three lithotypes is reported in table 4.

In order to investigate the microstructure of lithotypes, Mercury Intrusion Porosimetry (MIP) measurements were performed in the range from 100-0.01  $\mu\text{m}$  on 1  $\text{cm}^3$  stone specimens according to the procedure described in [28].

For Atomic Force Microscopy (AFM) analysis of surface roughness, a Solver Pro AFM microscope (NT-MDT Spectrum Instruments) was employed, using a silicon cantilever with a tip of 14-16  $\mu\text{m}$  height (NSG10, NT-MDT) and tip curvature radius of 10 nm at a resonant frequency of 140-390 KHz. Measurements were performed in tapping mode at 0.6 Hz scan rate, with 2 scans of a 0.5x0.5  $\mu\text{m}$  area. The acquired images were elaborated through the Nova SPM software (NT-MDT).

The total open porosity, average pore diameter and surface roughness of the three lithotypes are reported in table 1.

**Table 1.** Open porosity, Average pore diameter and Surface roughness (root mean square, RMS) of the three lithotypes.

Stone type	Open porosity (vol.%)	Average pore diameter ( $\mu\text{m}$ )	RMS Roughness (nm)
Apuan Marble	0.7a	0.08a	6 <sup>1</sup>
Balegem	9.9 $\pm$ 0.8	0.28 $\pm$ 0.06	38 $\pm$ 8
Obernkirchen	24.1 $\pm$ 0.1	0.8 $\pm$ 0.3	10 $\pm$ 9

<sup>1</sup> In the case of Apuan marble, measurements were only carried out on one specimen.



**Figure 1.** Photographs of Apuan marble (A), Balegem limestone (B) and Obernkirchen sandstone (C) prism specimens (5x5x2 cm).

### 2.2. Nanocomposites

The two nanocomposite formulations, hereafter referred to as WNC and ANC, consist of  $\text{TiO}_2$  nanoparticles dispersed in alkylalkoxysilane reactive sols. Their properties are summarized in table 2. The alkyl groups provide the coatings with hydrophobic properties, while  $\text{TiO}_2$  nanoparticles at low concentration are introduced to impart photocatalytic and self-cleaning properties.

The protective effectiveness and the general properties of these products have already been assessed in previous studies [29,30]. Upon solvent evaporation, the sol-gel condensation turns the alkylalkoxysilane precursors into cross-linked organosilica networks, their adhesion onto stone substrates being the result of both noncovalent (hydrogen bonding and dipolar interactions of the mineral surface with unreacted silanol groups, ionic interactions involving protonated amine in WNC) and covalent (sol-gel condensation with surface silanols of silicate stones) interactions.

In order to characterize the rheological behaviour of the products, a CV0 120 Rheometer (Bohlin Instruments Vertrieb GmbH) was employed, using a cone-plate configuration (1° angle, 40 mm diameter) with 0.03 mm gap. The measurements were conducted for 3 minutes under 0.01-3 Pa stress at 20 °C. Since the products exhibited a shear-thinning behaviour, the value of viscosity measured in the low shear rate region around 4 s<sup>-1</sup> was assumed to be representative of the rheological behaviour of the products in a capillary flow regime.

Particle size was measured on a 90 Plus Dynamic Laser Light Scattering instrument (Brookhaven Instruments Corporation) equipped with a 35-mW Laser and an Avalanche photodiode detector collecting the scattered light at 90°.

**Table 2.** Main chemical properties of the two nanocomposites.

	WNC	ANC
solvent	water	2-propanol
matrix former	<i>oligo-aminoalkyl alkoxysilane</i>	<i>monomeric alkylalkoxysilane</i>
dry matter in formulation (wt%)	15	40
density (g/cm <sup>3</sup> )	1.03	0.84
viscosity (mPa·s)	12	6
pH	4.5	-
TiO <sub>2</sub> (ppm)	9600	1200
TiO <sub>2</sub> particle size (nm)	106	25

### 2.3. Treatment procedure

Three 5x5x2 cm specimens per each lithotype and treatment were prepared. The stone specimens were gently polished with abrasive paper (P180 carborundum paper), kept in deionized water for an hour in order to remove any excess of soluble salts, dried in oven for 48 hours at 50°C and finally stored in a silica gel desiccator at room temperature for another 24 hours. The nanocomposites were applied by capillary absorption using a filter paper pad saturated with the treating material, according to the EN 16581:2014 protocol [31], for 6 hours. In order to determine the amount of dry matter applied, all specimens were weighed before the treatment and then after 1 month, which was considered as a sufficient time for the sol-gel reaction to occur. The amounts of absorbed dry matter as determined 1 month after the application are reported in table 3.

**Table 3.** Dry matter (mg/cm<sup>2</sup>) absorbed by lithotypes treated with WNC/ANC.

	WNC	ANC
Apuan marble	<0.01	0.5±0.2
Balegem	6±3	10±2
Obernkirchen	7±1	20±4

Each product was also cast on glass slides (25x75 mm) that had been previously treated with Piranha solution (conc. H<sub>2</sub>SO<sub>4</sub> and 30% H<sub>2</sub>O<sub>2</sub> in 3:1 volume ratio) in order to increase the amount of reactive silanol groups on the glass surface. The slides were kept under saturated solvent atmosphere until complete evaporation of the solvent and formation of a thin film, and then stored under the same conditions until the electrokinetic measurement was performed.

### 2.4. Water absorption measurements



Capillary water absorption was measured up to 96 h following the EN Standard Protocol [32, 33]. The relative capillary index as defined in eq. 2:

$$IC_{rel} = \frac{\text{integral}_t}{\text{integral}_{nt}}, \quad (2)$$

that is, the ratio of the absorption integrals of treated and untreated specimens, was used to compare the water absorption behaviour of treated and untreated stones.

### 2.5. Static contact angle measurements

Static contact angle ( $\theta$ ) measurements were performed on 15 areas for each specimen, according to the EN Standard Protocol [34], using an OCA (Optical Contact Angle) 20 PLUS (DataPhysics, Germany) equipment, with a drop volume of 5  $\mu\text{l}$ , 10 seconds after drop deposition. The test was carried out before and after the application of the treatments. The increase in contact angle from untreated to treated specimens ( $\Delta\theta = \theta_t - \theta_{nt}$ ) was assumed as parameter representing the reduction of surface wettability.

### 2.6. Streaming current measurements

Streaming current measurements on untreated/treated lithotypes and glass slides were performed using SURPASS Electrokinetic analyser (Anton Paar GmbH), with a measuring cell covering an area of 25x5 mm.  $10^{-3}$  M KCl in ultrapure water (18.2 M $\Omega$ ·cm) was used as electrolyte. In each measurement, four pressure ramps from 0-400 mbar were applied and the apparent zeta ( $\zeta$ ) potential was calculated from the slope of streaming current vs. pressure, according to the Smoluchowski eq. 1. Here the apparent  $\zeta$  potential was considered since in tangential electrokinetic measurements performed on a porous substrate the ionic conductivity within the porous structure and in the stagnant layer (shallows of the outer rough surface lying below the slip plane) contributes to the observed streaming current. While this contribution is difficult to evaluate by streaming potential measurements, it can be accounted for by performing streaming current measurements at different heights of the gap between the measuring cell surfaces [35]. Unfortunately, the adjustable gap cell required for such measurement is not suited for the analysis of large specimens such as the natural stone samples of the present study. Nevertheless, the apparent  $\zeta$  potential considered hereafter, though not accurate for describing the average surface charge density of such samples, is still a useful parameter to evaluate the extent of modifications induced by the application of a treatment modifying both the outer stone surface and, to some extent, the pore walls. The isoelectric point (IEP), i.e. the pH value at which  $\zeta=0$ , was determined by performing a sequence of measurements at slightly different pH values by means of an automatic titrator. Treated lithotypes and glass slides were analysed 1 month after the application of the products in order to allow for the formation of a seemingly stable gel network.

The shift of the isoelectric point relative to the *untreated* lithotype ( $\Delta\text{IEP}$ ) is given in eq. 3:

$$\Delta\text{IEP} = \frac{\text{IEP}_t - \text{IEP}_{nt}}{\text{IEP}_{nt}}, \quad (3)$$

where  $\text{IEP}_t$  is the isoelectric point of the treated lithotype and  $\text{IEP}_{nt}$  that of the untreated lithotype.

Then, in order to explore the possibility of using electrokinetic data for a quantitative estimation of the extent of surface modification produced by the two coatings, the shift of the isoelectric point was normalized according to eq. 4:

$$\text{ISM} = \frac{|\text{IEP}_t - \text{IEP}_{nt}|}{|\text{IEP}_s - \text{IEP}_{nt}|}, \quad (4)$$

where ISM, standing for Index of Surface Modification, is an empirical parameter evaluating the change in surface properties with respect to the untreated lithotype and  $\text{IEP}_s$  is the isoelectric point of the coating applied on glass slides.

## 3. Results

### 3.1. Electrokinetic analysis of untreated lithotypes

Streaming current measurements were performed on the three untreated lithotypes at various pH within different ranges, depending on the chemical stability of each given stone, to obtain their respective isoelectric points (IEP, table 4); for this purpose, titration curves were drawn by fitting the zeta potential values calculated from the streaming current data (figure 2). Even though the electrokinetic behaviour of porous materials is the result of a variety of factors, including the influence of surface conductance [28] and the effect of surface roughness [36], the differences observed among IEPs can be seen to quite closely reflect the mineralogical composition of the lithotypes under study. This indicates that the isoelectric point may be a suitable parameter describing the chemical composition of stone surfaces. In particular, the isoelectric point of Obernkirchen, i.e. a stone largely consisting of quartz, is in good agreement with the values reported in literature for silica and layered silicates [37,38]. In the case of Apuan marble, which is almost pure calcite, a comparison with literature data concerning calcite samples showed only partial agreement [39]; however, upon performing the electrokinetic titration on a single crystal of calcite, an IEP value in close correspondence to that determined on the marble was obtained.

**Table 4.** Mineralogical composition (calcite+dolomite content, in mol%), values of  $\zeta$  potential at pH 7 and 5 (in mV) and isoelectric points (IEP, in pH units) of *untreated* lithotypes.

Stone type	calcite+dolomite <sup>1</sup> (mol%)	$\zeta$ (pH 7) (mV)	$\zeta$ (pH 5) (mV)	IEP (pH units)
Apuan marble	99.6	-60±4	-47±4	3.7±0.1
Balegem	53.1	-57±6	-48±8	3.0±0.3
Obernkirchen	1.2	-88±10	-73±5	2.1±0.2
Calcite monocrystal	100	-	-39	3.6

<sup>1</sup> from X-ray diffraction measurements [27]

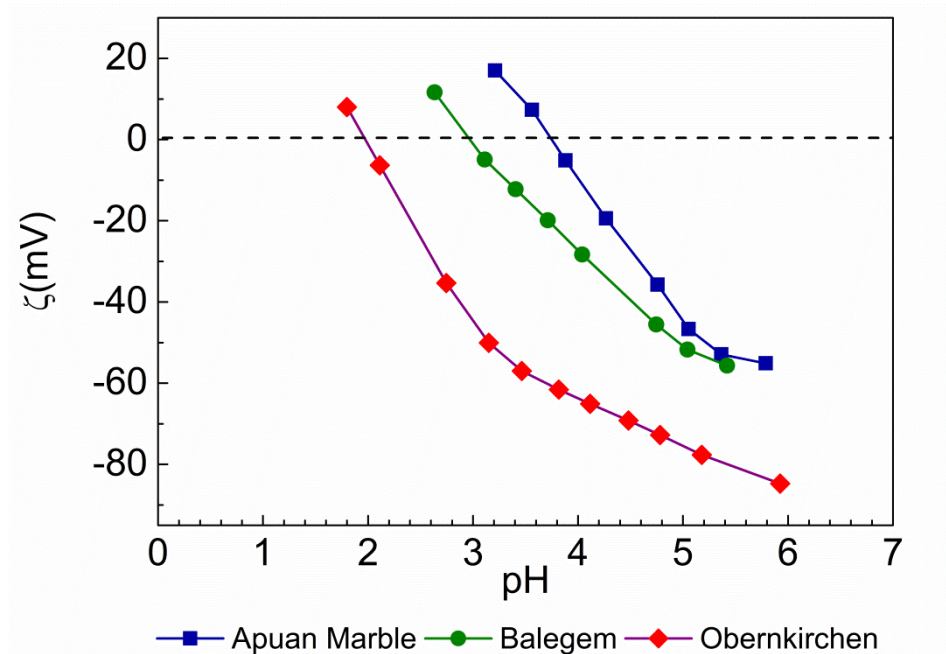


**Figure 2.** Example of titration curves expressing  $\zeta$  potential as a function of pH for the three lithotypes: Apuan marble, Balegem limestone and Obernkirchen sandstone.

### 3.2. Electrokinetic analysis of nanocomposites

From the results of the streaming current measurements on the two nanocomposite coatings applied onto glass slides (table 5) quite different IEPs were found, as expected from the different chemical structure of their components. In particular, the IEP of the WNC coating, which is based on an aminoalkyl trialkoxysilane precursor, lies in the alkaline pH region, in agreement with the presence of an amine group, its value being close to those reported in literature for other materials modified with aminosilane or aminosiloxane compounds [40,41]. On the other hand, the IEP of the ANC coating, based on an alkyl trialkoxysilane precursor, while being lower than that of WNC, turned out to be quite higher than those reported elsewhere for similar compounds [42]; this mismatch may depend on the different surface density of slightly acidic silanol groups resulting from the alkoxy silane hydrolysis not followed by exhaustive sol-gel condensation. In an aqueous environment, silanols are in their hydrolysed form and bear a negative charge, thus contributing to reduce the  $\zeta$  potential (and the IEP) of the surface. Depending on the molecular structure of the precursor and on the experimental conditions upon coating application (temperature, humidity, presence of catalytically active acidic or basic species in the formulation or at the surface of the glass substrate that was pre-treated with piranha solution), the surface density of free silanol groups may change and the  $\zeta$  potential may be affected accordingly. In addition, the surface density of silanols may change over an extended period of time (much longer than the four weeks of ageing allowed here to stabilize the coating before performing the measurements), as the sol-gel hydrolysis and condensation reactions proceed. Finally, a possibly not negligible contribution of the TiO<sub>2</sub> nanoparticles to the electrokinetic properties of the nanocomposite film surface should also be considered. In fact, TiO<sub>2</sub> has an IEP of 6.2, higher than that of pure silica, and with little difference between the two most common crystalline forms anatase and rutile [43]. Streaming current measurements were thus performed also on coatings cast on glass slides from the respective TiO<sub>2</sub>-free silane dispersions. From the results of these measurements (not reported) no significant difference in electrokinetic behaviour could be detected between the nanocomposite and the respective TiO<sub>2</sub>-free silane-based material, possibly because of the low concentration of TiO<sub>2</sub> nanoparticles and/or because they are mainly embedded in the organosilica gel network.

**Table 5.** Isoelectric points (IEP, in pH units) of the two nanocomposites applied on glass slides.

Coating	IEP (pH units)
WNC	10.3±0.7
ANC	7.9±0.8

3.3. Electrokinetic analysis of treated lithotypes

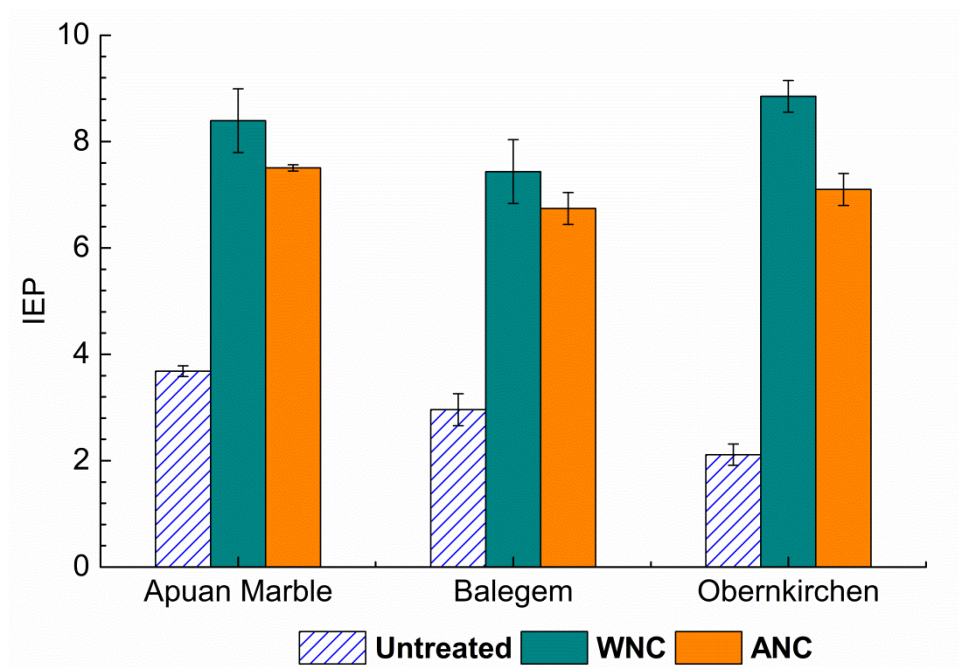
The results of the streaming current measurements on treated lithotypes (table 6 and figure 3) show that a remarkable increase in IEP takes place in all cases after the application of the treating products. As one may expect, the largest IEP changes were recorded for stones treated with WNC, the product providing a coating material with the highest inherent isoelectric point (table 5). Furthermore, the differences among the IEPs of untreated lithotypes (table 4) end up being partially masked after application of the products. For example, Obernkirchen stone, with its lowest IEP as untreated material, once treated shows nearly the same IEP values as the Apuan marble, a clear indication that the surface properties of the stones become dominated by those of the coating material. However, such differences are not completely cancelled out, and the IEP values of the treated stones are always lower than those measured on the coatings prepared on non-porous glass substrate. This suggests that the treating products do not succeed in producing a continuous and uniform coating layer on the mineral surface, including the pore walls of the outermost layer of the porous stone network.



**Table 6.** Values of  $\zeta$  potential at pH 7 (in mV) and isoelectric points (in pH units) of lithotypes before and after treatment with WNC/ANC.

Stone type	WNC				ANC			
	untreated <sup>1</sup>		treated		untreated <sup>1</sup>		treated	
	$\zeta$	IEP	$\zeta$	IEP	$\zeta$	IEP	$\zeta$	IEP
Apuan marble	-58±2	3.7±0.2	24±3	8.4±0.6	-62±3	3.7±0.1	7±6	7.51±0.06
Balegem	-54±5	2.8±0.3	9±5	7.7±0.2	-61±2	3.1±0.1	-22±10	6.4±0.3
Obernkirchen	-93 <sup>2</sup>	2.0±0.1	43 <sup>2</sup>	8.9±0.3	-85±10	2.2±0.2	1±1	7.1±0.3

<sup>1</sup> In order to take into account the inherent variability of lithotypes, electrokinetic data were always collected on the same specimens before and after the application of the coatings, hence two distinct sets of values are reported for untreated lithotypes. <sup>2</sup> For WNC on Obernkirchen stone,  $\zeta$  potential at pH 7 was only measured on one specimen.

**Figure 3.** Isoelectric points (IEP, in pH units) of the three lithotypes before and after treatment with WNC/ANC. Values for untreated lithotypes were obtained by averaging the two sets of values reported in table 6.

The extent to which the isoelectric point of stones is modified upon treatment may not linearly correlate with the actual fraction of surface coverage (SEM micrographs taken to assess the modification of surface morphology are available as Supplementary Materials, figures S1-S3), being more likely a complex parameter of surface modification also affected by the stone porosity features [35] and, when it applies, by the occurrence of chemical reactions between the stone and the coating material. Indeed, in the case of a porous substrate, the streaming current reflects not only the charge of the EDL from the external surface, but also the contribution from pore walls sensed by the tangential electrolyte flow. Thus, the penetration depth of the treating product and its effectiveness in generating a thin coating layer on the pore walls are additional factors affecting the streaming current measurements.

In our case, the results of electrokinetic measurements clearly indicate that, while both coating formulations succeeded in producing a significant modification of the surface chemical properties of the treated stones, the surface distribution of the coating material was less uniform than expected.

The relative variation  $\Delta\text{IEP}$  (eq. 3) for the six lithotype-treatment combinations reported in figure 4 does not appear to be correlated in a simple manner with the amount of product applied. In particular, in the case of ANC, a large difference in dry matter from Apuan marble to Balegem stone only corresponds to a negligible increase in  $\Delta\text{IEP}$ , while a comparable increase in the amount of product from Balegem and Obernkirchen gives rise to a comparatively large increase of  $\Delta\text{IEP}$ ; similarly, in the case of WNC, a minor increase of dry matter from Balegem to Obernkirchen results in a large increase in  $\Delta\text{IEP}$ , actually much larger than that recorded from Apuan marble to Balegem in spite of a higher increase in dry matter.

The two products indeed show markedly different penetration ability, as it is possible to infer from the amount of absorbed dry matter upon treatment (table 3). WNC has a limited penetration and tends to accumulate on the stone surface, leading to a significant increase in IEP at a comparatively low amount of product applied (figure 4). By contrast, the higher penetration of ANC results in a tendency to saturate stone porosity, so that a larger amount of product is needed to increase the isoelectric point of the stone surface, as it is especially clear when considering the trend from Apuan marble to Balegem stone (figure 4).

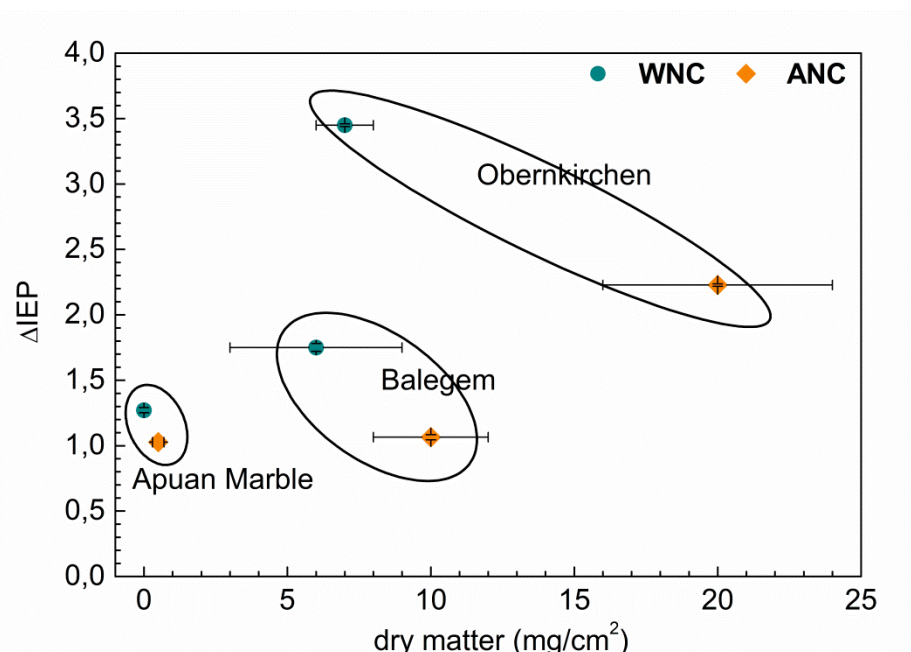


**Figure 4.** Correlation between dry matter ( $\text{mg}/\text{cm}^2$ ) and  $\Delta\text{IEP}$  (eq. 3) for lithotypes after treatment with WNC/ANC.

This evidence highlights the complexity of the picture resulting from the contribution of a multiplicity of factors in determining the extent of surface modification, in terms of both the amount of product actually deposited on the surface and the homogeneity of deposition. In particular, among the factors that are most likely to contribute are (i) the different chemical composition of the alkylalkoxysilane sols, resulting in possibly different reactivity and surface charge of organosilica nanogel particles that are likely to be present along with monomeric and oligomeric silanes, (ii) the different size of NPs dispersed in the two sols (table 2); (iii) the different porosity, average pore diameter and surface roughness of lithotypes (table 1) and (iv) their different chemical composition, resulting in different surface charge and specific chemical interaction (covalent or hydrogen bonding) with the sols.

The lower penetration of WNC may be tentatively explained as the result of incipient deposition of nanoparticles onto the outer surface, due to the presence of cationic ( $\text{IEP}=10.3$ , table 5) and reactive organosilica particles generated by sol-gel partial condensation of the aminated alkylalkoxysilane precursor. It is likely that such particles readily produce a monolayer on the negatively charged stone surface (more so in the case of Obernkirchen stone, whose IEP is lower

than that of the other two stones), which may prevent further absorption and penetration of the product if the stone porosity and pore size distribution are small enough to result in pore clogging, as it seems to be the case for WNC on Apuan marble. Indeed, since the  $\text{TiO}_2$  particle size in WNC is larger than the average pore size in Apuan marble (table 1, table 2), it is reasonable to assume that this component of the nanocomposite formulation does not penetrate into the pores and remains on the stone surface. Further to that, the hydrophobization resulting from the incipient modification of the outer stone surface may counteract further absorption and dry matter deposition. Then, additional contributions to the penetration effectiveness may result from the different degree of condensation (see particle size in table 2) and, albeit to a lower extent, the different viscosity of the matrix-forming alkylalkoxysilane sols.

In order to attempt a quantitative estimation of the extent of surface modification produced by the two coatings, the Index of Surface Modification (ISM) calculated from the isoelectric points of both stones and coatings (eq. 4) was considered. In accordance with its definition, ISM is a dimensionless parameter that does not depend on the inherent isoelectric points of different coatings, thus making it possible to establish a comparison between them. The validity of this approach was assessed by considering possible correlations of ISM with the reduction of capillary water absorption and surface wettability of treated stones, which are both dependent on the extent of surface hydrophobization. The definition of ISM rests on the assumption that, since films on glass slides make up less heterogeneous surfaces compared to treated stones, their IEP values ( $\text{IEP}_s$ ) may be expected to approximate those of the corresponding products more closely than the values measured on treated stones ( $\text{IEP}_t$ ). Hence, it was assumed that  $|\text{IEP}_s - \text{IEP}_{nt}| > |\text{IEP}_t - \text{IEP}_{nt}|$  or, equivalently,  $0 < \text{ISM} < 1$ , with 0 indicating no modification with respect to the untreated stone and 1 representing the virtual limit condition where the treated stone is homogeneously covered by the coating and behaves in the same way as the product film on glass slides.

The ISM values of ANC turn out to be higher than those of WNC (table 7), yet while on Apuan marble the difference is relevant, on Balegem and Obernkirchen stones it is far less so. Moreover, both products display the lowest ISM values on Balegem stone and higher values on Obernkirchen, whereas in the case of Apuan marble the trend is different: ANC exhibits a value comparable to that seen on Obernkirchen, while the value for WNC is significantly lower. The differences between the two products can be interpreted in the sense that ANC gives rise to a more homogeneous modification of stone surfaces compared to the other product. However, on Balegem and Obernkirchen stones the difference is rather small and may well fall within the experimental error. The lowest ISM values found on Balegem may be ascribed to the higher nanoscale roughness of this stone (table 1), which is likely to produce a less effective surface coverage.

**Table 8.** Absorption integrals (in  $\text{g}\cdot\text{cm}^{-2}\cdot\text{s}^{0.5}$ ) of *untreated* ( $\text{integral}_{nt}$ ) vs. *treated* ( $\text{integral}_t$ ) lithotypes and  $\text{IC}_{rel}$  values ( $=\text{integral}_t/\text{integral}_{nt}$ ).

Stone type	WNC			ANC		
	untreated	treated		untreated	treated	
	$\text{integral}_{nt}$	$\text{integral}_t$	$\text{IC}_{rel}$	$\text{integral}_{nt}$	$\text{integral}_t$	$\text{IC}_{rel}$
Apuan marble	$1.82\pm0.07$	$1.3\pm0.1$	$0.69\pm0.05$	$1.8\pm0.2$	$0.17\pm0.09$	$0.09\pm0.05$
Balegem	$98\pm13$	$15\pm4$	$0.15\pm0.04$	$76\pm4$	$5.2\pm0.4$	$0.068\pm0.003$
Obernkirchen	$121\pm4$	$15\pm5$	$0.12\pm0.04$	$124\pm4$	$6\pm1$	$0.05\pm0.01$

In apparent agreement with the ISM data, the results of water absorption (table 8) and static contact angle (table 9) measurements show that ANC is more effective than WNC, and particularly so in reducing water absorption that is likely to be more suitable than the static contact angle to assess the effectiveness of treatments, indicating the penetration and coverage of the outermost layer

of pore walls. The difference between the two products is relevant in the case of Apuan marble and increasingly smaller for Balegem and Obernkirchen stones. Similarly, the difference between the products in the static contact angle with water of treated vs. untreated lithotypes ( $\Delta\theta$ ) is only evident in the case of Apuan marble, where ANC imparts to the surface a higher hydrophobic character with respect to WNC, while it is totally negligible for the other two stones.

**Table 9.** Static contact angles ( $\theta$ , in degrees) of *untreated* ( $\theta_{nt}$ ) vs. *treated* ( $\theta_t$ ) lithotypes and  $\Delta\theta$  values ( $=\theta_t-\theta_{nt}$ ).

Stone type	WNC			ANC		
	untreated	treated	$\delta\theta$	untreated	treated	$\Delta\theta$
	$\theta_{nt}$	$\theta_t$		$\theta_{nt}$	$\theta_t$	
Apuan marble	53±4	129±13	76±13	51±1	141±2	92±2
Balegem	32±3	134±15	101±16	36±1	141±2	106±3
Obernkirchen	21±3	140±4	119±5	17±7	137±1	119±6

A correlation between ISM values for each coating-stone system and the corresponding  $IC_{rel}$  values can be made by inspection of figure 5. In fact, for each lithotype, the lowest  $IC_{rel}$  value was obtained for the specimen treated with ANC, the formulation showing the highest ISM value. In particular, the large difference between the products in terms of  $IC_{rel}$  observed on Apuan marble corresponds to a comparatively large difference in terms of ISM.

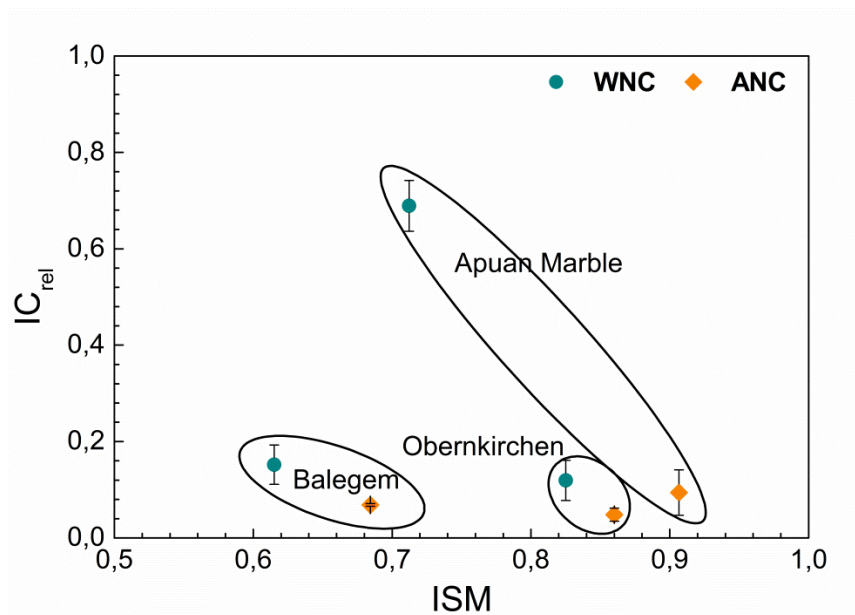


**Figure 5.** Correlation between Index of Surface Modification (ISM, eq. 4) and  $IC_{rel}$  (see section 2.4) for lithotypes after treatment with WNC/ANC.

Consistent with the observations about  $IC_{rel}$ , the trend of  $\Delta\theta$  values for each lithotype also corresponds rather well to that observed for ISM (figure 6). In particular, for Apuan marble, the large difference in  $\Delta\theta$  between WNC and ANC reflects an equally large difference in ISM, while the limited to negligible variation observed for Balegem and Obernkirchen corresponds to a similarly small variation in  $\Delta\theta$ . Finally, it can be observed that, on Apuan marble, both coatings produce an increase in static contact angle that is smaller than that observed on Balegem and Obernkirchen. This deviation may be tentatively ascribed to the much lower porosity of marble, leading to a rather effective coverage of the outer stone surface (and thus high ISM value) but a less effective



hydrophobic modification at corresponding low surface energy coating material due to the lower surface roughness of stone and the resulting lower contribution to the measured contact angle by the Cassie-Baxter state [44,45].

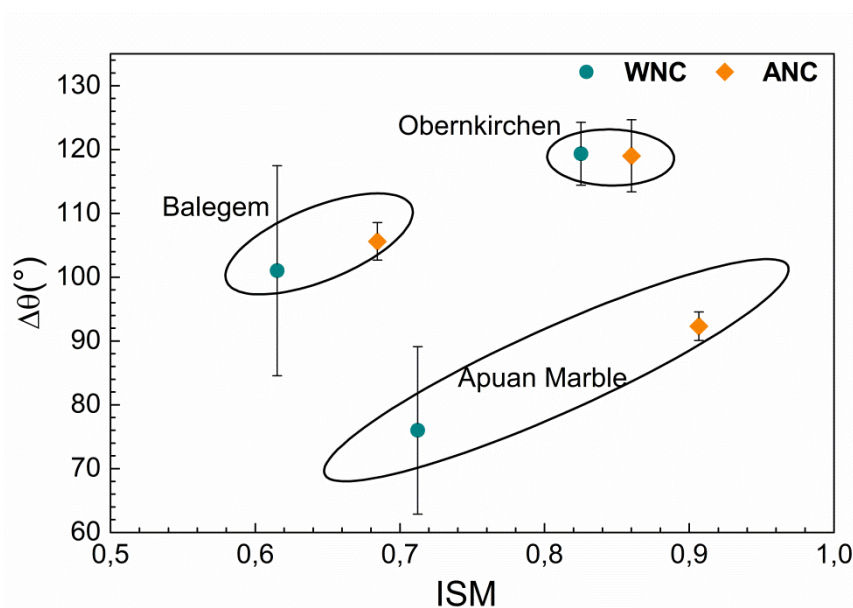


**Figure 6.** Correlation between Index of Surface Modification (ISM, eq. 4) and  $\Delta\theta$  (see section 2.5) for lithotypes after treatment with WNC/ANC.

In summary, the empirical ISM parameter, which was anticipated to reflect the extent of surface modification, showed indeed a correlation with the reduction of water absorption and surface wettability of treated stones. In particular, on Balegem and Obernkirchen stones, where the two coatings provided similar results in terms of ISM, similar values of  $IC_{rel}$  and  $\Delta\theta$  were also observed, while their different interaction with water observed on Apuan marble was also accompanied by a greater difference in ISM. In this latter case, ANC was seen to produce a greater reduction in capillary water absorption and a greater increase in static contact angle as compared to the other product. Such difference reflects, though not exclusively, those seen in the interaction of the products with the stone surface and in their penetration effectiveness, which was earlier discussed with reference to the respective amounts of absorbed dry matter. In particular, the low porosity and low pore diameter of marble, alongside the cationic surface charge (higher IEP with respect to ANC) and larger-sized particles in the WNC formulation, result in poorer penetration of this product and are likely responsible for the less homogeneous stone surface modification and less effective hydrophobization achieved.

#### 4. Conclusions

Electrokinetic measurements, being sensitive to molecular level modifications and yet averaging the response over a macroscopic sized surface area, provide information useful for a more accurate understanding of the different contributions (chemistry and morphology of stone and nanocomposite product formulation) to the ultimate performance of a coating material. In particular:

- electrokinetic analysis based on streaming current measurements was shown to be a sensitive and effective tool to characterize the modification of the surface properties of different natural stones upon application of coating materials;
- a correlation was found between the extent of surface modification (according to the empirical ISM parameter) and the effectiveness of the products as determined by the reduction of water absorption by capillarity and of surface wettability for the six investigated lithotype-nanocomposite coating combinations;



- significant differences were observed between the low porosity Apuan marble and the other two more porous lithotypes, as the former prevents to a large extent penetration of more viscous fluids and possibly of nanoparticles, while the difference between products is, to a good extent, levelled out in the case of the most porous lithotypes as a result of product absorption into the stone matrix;

In summary, the ISM parameter based on streaming current measurements was shown to provide quantitative information on the quality and uniformity of the modification produced by the application of a surface treatment material on a porous substrate when a very thin (not occlusive of the pore structure) coating layer is required. In particular, the effectiveness of the treatment correlates well with the ISM data unless saturation, that is exhaustive coverage of the surface including the pore walls of the outermost layer probed by the streaming current measurement, is achieved.

Further useful and more general applications are foreseen, concerning the characterization of surface treatments based on multicomponent formulations such as e.g. micro- or nanocomposite coating materials in which the surface properties may be strongly influenced by the preferential segregation of one of the components at the outer coating surface.

**Supplementary Materials:** The following are available online at [www.mdpi.com/xxx/s1](http://www.mdpi.com/xxx/s1), Figure S1: SEM images of Apuan marble: A) untreated; B) treated with WNC; C) treated with ANC. Figure S2: SEM images of Balegem stone: A) untreated; B) treated with WNC; C) treated with ANC. Figure S3: SEM images of Obernkirchen stone: A) untreated; B) treated with WNC; C) treated with ANC.

**Author Contributions:** Conceptualization, Marco Roveri and Valter Castelvetro; Data curation, Marco Roveri; Funding acquisition, Simona Raneri, Valter Castelvetro and Lucia Toniolo; Investigation, Marco Roveri, Simona Raneri and Sabrina Bianchi; Supervision, Francesca Gherardi and Lucia Toniolo; Writing – original draft, Marco Roveri; Writing – review & editing, Simona Raneri, Francesca Gherardi and Valter Castelvetro.

**Funding:** This research was funded by the EU Horizon 2020 programme, grant number 646178 (“NanoCathedral - Nanomaterials for conservation of European architectural heritage developed by research on characteristic lithotypes”). S.R. was also funded by the University of Pisa, PRA project number 2018\_41.

**Acknowledgments:** The authors wish to thank ChemSpec Srl (Italy) and Colorobbia Consulting Srl (Italy) for supplying the nanomaterials, Ms. Matea Ban from Technical University of Vienna for the Mercury Intrusion Porosimetry measurements, Dr. Thomas Luxbacher from Anton Paar GmbH (Austria) for initial scientific advice, and Prof. Marco Lezzerini from the University of Pisa for performing X-ray diffraction measurements and for providing the calcite monocrystal sample.

**Conflicts of Interest:** The authors declare no conflict of interest.

## References

1. Snethlage, R. Stone Conservation. In: *Stone in architecture: properties, durability*, 5th ed., Siegesmund, S., Snethlage, R., Eds.; Springer Verlag, Berlin-Heidelberg, Germany, 2014; pp. 415-550, ISBN 978-3-662-49573-5.
2. Della Volpe, C.; Penati, A.; Peruzzi, R.; Siboni, S.; Toniolo, L.; Colombo, C. Combined effect of roughness and heterogeneity on contact angles: The case of polymer coating for stone protection. *J. Adhes. Sci. Technol.* **2000**, *14*, 273-299. <https://doi.org/10.1163/156856100742555>.
3. De Ferri, L.; Lottici, P.P.; Lorenzi, A.; Montenero, A.; Salvioli-Mariani, E. Study of silica nanoparticles - polysiloxane hydrophobic treatments for stone-based monument protection. *J. Cult. Herit.* **2011**, *12*, 356-363. <https://doi.org/10.1016/j.culher.2011.02.006>.
4. Fermo, P.; Cappelletti, G.; Cozzi, N.; Padeletti, G.; Kaciulis, S.; Brucale, M.; Merlini, M. Hydrophobizing coatings for cultural heritage. A detailed study of resin/stone surface interaction. *Appl. Phys. A* **2014**, *116*, 341-348. <https://doi.org/10.1007/s00339-013-8127-z>.
5. Crupi, V.; Fazio, B.; Gessini, A.; Kis, Z.; La Russa, M.F.; Majolino, D.; Masciovecchio, C.; Ricca, M.; Rossi, B.; Ruffolo, S.A.; Venuti, V. TiO<sub>2</sub>-SiO<sub>2</sub>-PDMS nanocomposite coating with self-cleaning effect for stone material: Finding the optimal amount of TiO<sub>2</sub>. *Constr. Build. Mater.* **2018**, *166*, 464-471. <https://doi.org/10.1016/j.conbuildmat.2018.01.172>.
6. Lettieri, M.; Masieri, M. Surface characterization and effectiveness evaluation of anti-graffiti coatings on highly porous stone materials. *Appl. Surf. Sci.* **2014**, *288*, 466-477. <https://doi.org/10.1016/j.apsusc.2013.10.056>.
7. La Russa, M.F.; Rovella, N.; Alvarez De Buergo, M.; Belfiore, C.M.; Pezzino, A.; Crisci, G.M.; Ruffolo, S.A. Nano-TiO<sub>2</sub> coatings for cultural heritage protection: The role of the binder on hydrophobic and self-cleaning efficacy. *Prog. Org. Coat.* **2016**, *91*, 1-8. <https://doi.org/10.1016/j.porgcoat.2015.11.011>.
8. Xiong, Q.; Baychev, T.G.; Jivkov, A.P. Review of pore network modelling of porous media: Experimental characterisations, network constructions and applications to reactive transport. *J. Contam. Hydrol.* **2016**, *192*, 101-117. <https://doi.org/10.1016/j.jconhyd.2016.07.002>.
9. Doehne, E. Price, C.A. *Stone Conservation. An Overview of Current Research*, 2nd ed.; The Getty Conservation Institute, Los Angeles, CA, 2010, ISBN 978-1-60606-046-9.
10. Andreotti, S.; Franzoni, E.; Fabbri, P. Poly(hydroxyalkanoate)s-based hydrophobic coatings for the protection of stone in cultural heritage. *Materials* **2018**, *11*, 11010165. <https://doi.org/10.3390/ma11010165>.
11. T. Luxbacher, *The Zeta Guide: Principles of the Streaming Potential Technique*, Anton Paar GmbH, Graz, 2014.
12. von Smoluchowski, M. Contribution à la théorie de l'endosmose électrique et de quelques phénomènes corrélatifs. *Bull. Int. Acad. Sci. Cracovie, Cl. Sci. Math.* **1903**, 182-99.
13. Ristić, T.; Hribernik, S.; Fras-Zemljič, L. Electrokinetic properties of fibres functionalised by chitosan and chitosan nanoparticles. *Cellulose* **2015**, *22*, 3811-3823. <https://doi.org/10.1007/s10570-015-0760-6>.
14. Ripoll, L.; Bordes, C.; Marote, P.; Etheve, S.; Elaissari, A.; Fessi, H. Electrokinetic properties of bare or nanoparticle-functionalized textile fabrics. *Colloids Surf., A* **2012**, *397*, 24-32. <https://doi.org/10.1016/j.colsurfa.2012.01.022>.
15. Déon, S.; Fievet, P.; Osman Doubad, C. Tangential streaming potential/current measurements for the characterization of composite membranes. *J. Membr. Sci.* **2012**, *423-424*, 413-421. <https://dx.doi.org/10.1016/j.memsci.2012.08.038>.
16. Wang, Y.; Guo, L.; Ren, L.; Yin, S.; Ge, J.; Gao, Q.; Luxbacher, T.; Luo, S. A study on the performance of hyaluronic acid immobilized chitosan film. *Biomed. Mater.* **2009**, *4*, 035009. <https://doi.org/10.1088/1748-6041/4/3/035009>.
17. Heberling, F.; Trainor, T.P.; Lützenkirchen, J.; Eng, P.; Denecke, M.A.; Bosbach, D. Structure and reactivity of the calcite-water interface. *J. Colloid Interface Sci.* **2011**, *354*, 843-857. <https://doi.org/10.1016/j.jcis.2010.10.047>.
18. Kershner, R.J.; Bullard, J.W.; Cima, M.J. Zeta Potential Orientation Dependence of Sapphire Substrates. *Langmuir* **2004**, *20*, 4101-4108. <https://doi.org/10.1021/la036268w>.
19. Laumann, S.; Micić, V.; Lowry, G.V.; Hofmann, T. Carbonate minerals in porous media decrease mobility of polyacrylic acid modified zero-valent iron nanoparticles used for groundwater remediation. *Environ. Poll.* **2013**, *179*, 53-60. <https://doi.org/10.1016/j.envpol.2013.04.004>.

20. Adamczyk, Z.; Sadlej, K.; Wajnryb, E.; Nattich, M.; Ekiel-Jezewska, M.L.; Bławdziewicz, J. Streaming potential studies of colloid, polyelectrolyte and protein deposition. *Adv. Colloid Interface Sci.* **2010**, *153*, 1-29. <https://doi.org/10.1016/j.cis.2009.09.004>.
21. Szymczyk, A.; Dirir, Y.I.; Picot, M.; Nicolas, I.; Barrière, F. Advanced electrokinetic characterization of composite porous membranes. *J. Membr. Sci.* **2013**, *429*, 44-51. <https://doi.org/10.1016/j.memsci.2012.11.076>.
22. Cerepi, A.; Loisy, C.; Toullec, R.; Burlot, R.; Galaup, S.; Schmutz, M. Electrical behaviour of saturated and unsaturated geological carbonate porous systems. *Stud. Surf. Sci. Catal.* **2006**, *160*, 713-719.
23. Vdović, N.; Bišćan, J. Electrokinetics of natural and synthetic calcite suspensions. *Colloids Surf., A* **1998**, *137*, 7-14. [https://doi.org/10.1016/S0927-7757\(97\)00179-9](https://doi.org/10.1016/S0927-7757(97)00179-9).
24. Kanellopoulou, D.G.; Koutsoukos, P.G. The calcitic marble/water interface: Kinetics of dissolution and inhibition with potential implications in stone conservation. *Langmuir* **2003**, *19*, 5691-5699. <https://doi.org/10.1021/la034015x>.
25. Zhao, Z.; Wang, G. Surface electrical property and adsorption performance of Maifan stone, *Heilongjiang Daxue Ziran Kexue Xuebao* **2007**, *24*, 357-360. Language: Chinese
26. Falchi, L.; Balliana, E.; Izzo, F.C.; Agostinetto, L.; Zendri, E. Distribution of nanosilica dispersions in Lecce stone. *Sciences at Cà Foscari* **2013**, *1*, 39-46. <https://arca.unive.it/retrieve/handle/10278/38112/28517/441-2182-1-PB.pdf>
27. Lezzerini, M.; Marroni, M.; Raneri, S.; Tamayo, S.; Narbona, B.; Fernández, B.; Weber, J.; Ghaffari, E.; Ban, M.; Rohatsch, A. D1.5 – Mapping of stones and their decay: Part I - Natural stone test methods, NanoCathedral project Grant Agreement no. 646178 - confidential deliverable 2017, pp. 8-16.
28. Giesche, H. Mercury Porosimetry: A General (Practical) Overview. *Part. Part. Syst. Charact.* **2006**, *23*, 9-19. <https://doi.org/10.1002/ppsc.200601009>.
29. Roveri, M.; Gherardi, F.; Goidanich, S.; Niccolai, L.; Dami, V.; Toniolo, L. Use of nanomaterials for the protection of historic stone architecture: laboratory methods for the evaluation and investigation of photocatalytic activity. In Proceedings of the 4th WTA International PhD Symposium, Delft, Netherlands, 13-16 September 2017; Quist, W.J., Granneman, S.J.C., van Hees R.P.J., Eds., TU Delft, 2017, pp. 55-64.
30. Gherardi, F.; Roveri, M.; Goidanich, S.; Toniolo, L. Photocatalytic Nanocomposites for the Protection of European Architectural Heritage. *Materials* **2018**, *11*, 11010065. <https://doi.org/10.3390/ma11010065>.
31. EN 16581:2014. Conservation of cultural heritage - surface protection for porous inorganic materials - laboratory test methods for the evaluation of the performance of water repellent products. European Committee for Standardization: 2014.
32. EN 15801:2009. European Committee for Standardization: Conservation of cultural property - Test methods - Determination of water absorption by capillarity, 2009.
33. Peruzzi, R.; Poli, T.; Toniolo, L. The experimental test for the evaluation of protective treatments: A critical survey of the "capillary absorption index". *J. Cult. Herit.* **2003**, *4*, 251-254. [https://doi.org/10.1016/S1296-2074\(03\)00050-5](https://doi.org/10.1016/S1296-2074(03)00050-5).
34. EN 15802:2009. European Committee for Standardization Conservation of cultural property - Test methods - Determination of static contact angle, 2009.
35. Yaroshchuk, A.; Luxbacher, T. Interpretation of electrokinetic measurements with porous films: Role of electric conductance and streaming current within porous structure. *Langmuir* **2010**, *26*, 10882-10889. <https://doi.org/10.1021/la100777z>.
36. Schnitzer, C.; Ripperger, S. Influence of surface roughness on streaming potential method. *Chem. Eng. Technol.* **2008**, *31*, 1696-1700. <https://doi.org/10.1002/ceat.200800180>.
37. Kosmulski, M. Compilation of PZC and IEP of sparingly soluble metal oxides and hydroxides from literature. *Adv. Colloid Interface Sci.* **2009**, *152*, 14-25. <https://doi.org/10.1016/j.cis.2009.08.003>.
38. Alvarez-Silva, M.; Uribe-Salas, A.; Mirnezami, M.; Finch, J.A. The point of zero charge of phyllosilicate minerals using the Mular-Roberts titration technique. *Miner. Eng.* **2010**, *23*, 383-389. <https://doi.org/10.1016/j.mineng.2009.11.013>.
39. Vdović, N. Electrokinetic behaviour of calcite - The relation with other calcite properties. *Chem. Geol.* **2001**, *177*, 241-248. [https://doi.org/10.1016/S0009-2541\(00\)00397-1](https://doi.org/10.1016/S0009-2541(00)00397-1).
40. Hayes, R.A.; Böhmer, M.R.; Fokkink, L.G.J. Study of silica nanoparticle adsorption using optical reflectometry and streaming potential techniques. *Langmuir* **1999**, *15*, 2865-2870. <https://doi.org/10.1021/la980668f>.

41. Dussaud, A.D.; Breen, P.C.; Koczko, K. Characterization of the deposition of silicone copolymers on keratin fibers by streaming potential measurements. *Colloids Surf., A* **2013**, *434*, 102-109. <https://doi.org/10.1016/j.colsurfa.2013.04.071>.
42. Lee, C.H.; Park, S.H.; Chung, W.; Kim, J.Y.; Kim, S.H. Preparation and characterization of surface modified silica nanoparticles with organo-silane compounds. *Colloids Surf., A* **2011**, *384*, 318-322. <https://doi.org/10.1016/j.colsurfa.2011.04.010>.
43. Kosmulski, M. The significance of the difference in the point of zero charge between rutile and anatase, *Adv. Colloid Interface Sci.* **99** **2002**, 255-264. [https://doi.org/10.1016/S0001-8686\(02\)00080-5](https://doi.org/10.1016/S0001-8686(02)00080-5).
44. Cassie, A.B.D.; Baxter, S. Wettability of porous surfaces. *Trans. Faraday Soc.* **1944**, *40*, 546-551. <https://doi.org/10.1039/TF9444000546>.
45. Brugnara, M.; Degasperis, E.; Della Volpe, C.; Maniglio, D.; Penati, A.; Siboni, S.; Toniolo, L.; Poli, T.; Invernizzi, S.; Castelvetro, V. The application of the contact angle in monument protection: New materials and methods. *Colloids Surf., A* **2004**, *241*, 299-312. <https://doi.org/10.1016/j.colsurfa.2004.04.035>.